Theor Chem Acc (2012) 131:1152
DOI 10.1007/s00214-012-1152-8

REGULAR ARTICLE

How polarization damping affects ion solvation dynamics

Elvira Guàrdia · Ausias March Calvo · Marco Masia

Received: 29 April 2011 / Accepted: 23 September 2011 / Published online: 19 February 2012

Abstract In a recent paper (Sala et al. in J Chem Phys 133:234101, 2010), static properties of chloride in water have been addressed using a polarizable force field and by adding screening functions to damp short-range electrostatic interactions. In this contribution, we further explore the impact of damping polarizable interactions on system dynamics. To this end, results from Car–Parrinello molecular dynamics simulations have been used as benchmark for assessing the impact of damping schemes on the ion solvation dynamics of chloride in water. The results are of general validity, and the methodology could be easily implemented in *all methods* used to include polarization.

Keywords Polarization · Force field · Damping · Car–Parrinello · Ion solvation dynamics

Published as part of the special collection of articles: From quantum mechanics to force fields: new methodologies for the classical simulation of complex systems.

E. Guàrdia · A. M. Calvo
Departament de Física i Enginyeria Nuclear, Universitat Politècnica de Catalunya, Campus Nord B4-B5, 08034 Barcelona, Spain
e-mail: elvira.guardia@upc.edu

A. M. Calvo
e-mail: ausias.march@upc.edu

M. Masia (✉)
Dipartimento di Chimica, Istituto Officina dei Materiali del CNR, UOS SLACS, Università degli Studi di Sassari, Via Vienna 2, 07100 Sassari, Italy
e-mail: marco.masia@uniss.it

1 Introduction

It is widely accepted that the inclusion of polarization effects in force field molecular dynamics (MD) simulations is of high importance for studying both homogeneous and inhomogeneous systems [1–6]. The contribution of many body terms to the total interaction potential (neglected in non-polarizable empirical potentials) is known to vary with the systems, and it is not straightforward to assess it a priori [7]. It is certain, though, that a proper description of polarizable interactions represents the next milestone in force field development. In fact, even though dipolar interactions decay faster than Coulomb ones, they are responsible of interesting and non-negligible physical chemical properties; as an example, the anion surface propensity in water/air interfaces could be explained only by using polarizable force fields [8–11]. The same applies to solvation of highly charged cations: for lanthanides in water, it has been found that EXAFS and XANES spectra could be reproduced only by adding polarizability [12]. Besides these applications, strictly related to ions in water, the study of many different systems might be faced with polarizable force fields, for example, molten salts [13, 14], ionic liquids [15] and biosystems [16].

The most widespread methods to deal with polarization in MD simulations are the Drude oscillator model (or charge on spring), the fluctuating charge model and the Polarizable Point Dipoles method [5, 17, 18]. The latter has been applied in the present contribution; it should be stressed, though, that the conclusions of our study are of general validity and that they could be easily ported to any of the above-mentioned methods. The main focus of our research is to ascertain which features a polarizable force field should have in order to accurately describe the intermolecular potential. We believe that these aspects are important for developing next generation of force fields

that might be used to study, *inter alia*, heterogeneous systems in the presence of high electric fields.

Recently, many authors [19–24] have pointed out that one of the largest limitations of standard molecular-mechanics polarizable force fields lies in that the transferability of gas phase derived potentials to condensed phase is hindered by the absence of polarization exchange-coupling in classical models (since it is due to short-range electron cloud repulsion, it is also known as *Pauli effect* [25]). In 1981 Thole [26] published a seminal paper on the use of damping functions for hindering the so-called *intramolecular polarization catastrophe*, that is, the divergence of dipole moments causing the dynamics to breakdown. Although his results could be extended also to *intermolecular interactions*, only recently this approach has been used in MD simulations [27, 28]. This perspective guided one of us in pursuing a method to develop polarizable models, which could faithfully reproduce the electrostatic properties of simple systems such as ion-molecule (either water or carbon tetrachloride) dimers [17–22, 23]. The method was then extended to bulk systems [28], where we assessed the impact of damping short-range electrostatic interactions on static properties. A model system, namely a chloride ion in water, was studied by comparing force field and Car–Parrinello MD. We found that, while the structure (radial distribution function) is already well reproduced by using a low value for the polarizability (α_{Cl} = 3.2 Å^3) without damping, electrostatic properties are not. In particular we proved that, with such systems, the ion dipole moment is overestimated (broad dipole moment distribution, shifted to high values) and that the ion is characterized by a high polarization anisotropy. Finally we showed that all these quantities are well reproduced if gas-phase polarizability is used (α_{Cl} = 5.48 Å^3), together with damping functions. Recently, it has been pointed out that including short-range damping allows to reproduce thermodynamical properties of halide ions at interfaces [11]. It must be noticed that many authors suggest the use of low polarizabilities for halide in water, thus introducing implicitly the interaction with the electron density of surrounding molecules. With their approach, the polarizability at condensed phase would be smaller than that at gas phase. One weak point of this approach is that the polarization at intermediate distances is lower than expected, as highlighted by high-level quantum chemical calculations on a simple ion–water dimer [22]. On the other hand, our approach is based on the assumption that the ionic polarizability is the same as that at gas phase and that, using suitable damping functions, we account for the dynamical response of the anion to the electron density of the environment.

In this article we investigate the impact of using short-range damping functions on the dynamical properties of the systems. This is of particular interest mainly for people studying ion solvation dynamics. Indeed, these features are the focus of many experimental and theoretical studies such as in references [8, 9, 29–32, 33], to cite just the most outstanding ones. In particular the properties which are mostly observed/simulated are related to the ion (diffusion coefficients) and to its environment (rotational relaxation, exchange times and mechanism, etc). Since in the bulk, ionic and molecular polarization influences solvation shell dynamics [32–36], we focus on ion diffusion, characteristic exchange times of first shell water molecules and rotational dynamics. The manuscript is organized as follows: In Sect. 2 the computational approach used is explained, in Sect. 3 the results are discussed, and then, follow our conclusions in Sect. 4.

2 Computational details

2.1 Electrostatic damping

The total electrostatic energy of a system of charges and dipoles can be partitioned into different contributions arising from charge–charge, charge–dipole and dipole–dipole interactions plus the dipole polarization term:

$$\begin{aligned} U_{\mathrm{el}} &= U_{qq} + U_{q\mu} + U_{\mu\mu} + U_{\mathrm{dip}}^{\mathrm{pol}} \\ &= \sum_i \sum_{j>i} \left(q_i \hat{T}_{ij} q_j + \mu_i^{\alpha} \hat{T}_{ij}^{\alpha} q_j - q_i \hat{T}_{ij}^{\alpha} \mu_j^{\alpha} - \mu_i^{\alpha} \hat{T}_{ij}^{\alpha\beta} \mu_j^{\beta} \right) \\ &\quad + \frac{1}{2} \sum_{i=1}^{N_\mu} \boldsymbol{\mu}_i \cdot \hat{\alpha}_i^{-1} \cdot \boldsymbol{\mu}_i, \end{aligned} \tag{1}$$

where $\hat{\alpha}_i$ is the ith atom polarizability tensor; in the following discussion, we consider it to be isotropic, thus substituting the tensor with a scalar. In the above equation we have introduced the *electrostatic interaction tensors* $\hat{T}_{ij}$, $\hat{T}_{ij}^{\alpha}$ and $\hat{T}_{ij}^{\alpha\beta}$, which are useful for calculating, energies, forces and electric fields. Their functional form [28, 37] is given by:

$$\hat{T}_{ij} = [s_0(r)] \frac{1}{r} \tag{2}$$

$$\hat{T}_{ij}^{\alpha} = \nabla_{\alpha} \hat{T}_{ij} = -[s_1(r)] \frac{r_{\alpha}}{r^3} \tag{3}$$

$$\hat{T}_{ij}^{\alpha\beta} = \nabla_{\alpha} \hat{T}_{ij}^{\beta} = [s_2(r)] \frac{3 r_{\alpha} r_{\beta}}{r^5} - [s_1(r)] \frac{\delta_{\alpha\beta}}{r^3} \tag{4}$$

$$\begin{aligned} \hat{T}_{ij}^{\alpha\beta\gamma} = \nabla_{\alpha} \hat{T}_{ij}^{\beta\gamma} &= -[s_3(r)] \frac{15}{r^7} r_{\alpha} r_{\beta} r_{\gamma} + [s_2(r)] \frac{3}{r^5} \left(r_{\alpha} \delta_{\beta\gamma} + r_{\beta} \delta_{\alpha\gamma} \right. \\ &\quad \left. + r_{\gamma} \delta_{\alpha\beta} \right), \end{aligned} \tag{5}$$

where r_{α}, r_{β} and r_{γ} are the cartesian components of the vector $\mathbf{r} = \mathbf{r}_i - \mathbf{r}_j$ defining the distance (which norm is

$r = |\mathbf{r}|$) between particles i and j, and the Kronecker delta function $\delta_{\alpha\beta}$ returns 1 if $\alpha = \beta$ and 0 otherwise. The appropriate screening functions $s_n(r)$ describe the kind of interacting charges' distributions. In traditional point charge schemes the charge distribution is a delta function centered in $\mathbf{r}_i$ ($s_n(r) = 1$); some applications deal with smeared charges, and the screening functions are not unit, but rather a nonlinear function of the distance. It can be easily shown that, knowing $s_0(r)$, higher-order screening functions are recursively obtained applying

$$s_k(r) = s_{k-1}(r) - \frac{r}{2k-1}\frac{\partial}{\partial r}s_{k-1}(r). \quad (6)$$

The use of screening functions is well established both for the Ewald summation method (accounting for the periodic boundary conditions) and for electrostatic damping schemes. The latter arise naturally if one considers that the charges or dipoles are not points, but rather distributed according to same a priori assumed distribution. This is, indeed, a realistic situation when the molecules come "close enough". In the case of halide ions, it has been shown that "close enough" means ca. 4 Å [22, 23]. In this paper we studied both the exponential and the gaussian charge distributions, which have been shown to be the most promising; furthermore, they are easy to implement and they imply a negligible computational overhead (see [28] for further details).

Here we would like to stress that, although the polarizable point dipole scheme allows for more flexibility, the method could be easily extended to other schemes accounting for polarizability. In fact, the overall effect of damping functions is to screen the electric field for short-range interactions. Therefore, given that both in Drude oscillators and in fluctuating charges methods there are not dipoles, but only charge, it suffices to consider the damping of the tensors accounting for charge–charge interactions. Recently, the method has been implemented in CHARMM force field [38, 39], together with Drude oscillators.

2.2 Classical MD

Classical MD simulations were performed with an in-house program which will be let freely under request. The system is composed of 96 water molecules and one chloride anion. The size of system was chosen in order to compare with Car–Parrinello MD simulations; in fact, although the Ewald summation technique allows to deal with charged systems, according to our calculations, static and dynamical properties are slightly affected by the size of the simulation box.

The polarizable point dipole method has been used for accounting for polarization. For water we implemented the RPOL model [40]: The charges associated with each atom reproduce the water dipole moment at gas phase. On top of that, site polarizabilities are associated with each atom, which allow to obtain a dipole moment distribution at condensed phase peaked at ca. 2.6 D. The force field parameters are divided into seven models, differing among them for the value of chloride polarizability and for the type of the assumed charge distribution; the main features of these models are resumed in Table 1. The entire set of parameters for the force fields used are given in Tables I and II of [28].

Table 1 List of names and main features of the studied models

Model	Charge distribution	$\hat{\alpha}$ (Å^3)
A3.2-none	None	3.25
A3.2-gau	Gaussian	3.25
A4.0-gau	Gaussian	4.00
A5.5-gau	Gaussian	5.48
A3.2-exp	Exponential	3.25
A4.0-exp	Exponential	4.00
A5.5-exp	Exponential	5.48

See [28] for further details

In order to accelerate the computational time, the ASPC scheme [41] has been implemented. After having equilibrated the system at 298 K for 500 ps, we have run six NVE 1 ns simulations, starting from different initial configurations.

2.3 Car–Parrinello MD

Ab initio simulations have been performed, using the Car–Parrinello (CP) [42] scheme for propagating the wave-function and the ionic configurations as implemented in the `CPMD` package [43]. The BLYP density functional [44, 45] was used for the electronic structure calculations. The

Table 2 Diffusion coefficients for the chloride ion obtained from the mean square displacement (D_{msd}) and from the velocity autocorrelation function (D_{vacf})

Model	D_{msd} (10^{-9} m^2 s^{-1})	D_{vacf} (10^{-9} m^2 s^{-1})	T (K)
A3.2-none	0.67 (0.09)	0.72 (0.12)	299.1 (2.4)
A3.2-exp	0.78 (0.17)	0.86 (0.15)	297.0 (5.3)
A3.2-gau	0.83 (0.12)	0.74 (0.11)	307.0 (5.1)
A4.0-exp	1.11 (0.12)	1.10 (0.12)	305.4 (2.5)
A4.0-gau	0.87 (0.14)	0.93 (0.10)	298.6 (2.7)
A5.5-exp	1.12 (0.10)	1.22 (0.09)	295.2 (3.9)
A5.5-gau	0.78 (0.17)	0.85 (0.16)	291.5 (4.9)
CPMD	1.07	–	300.0

Values for classical MD are averaged over six NVE simulations (mean standard deviations in parenthesis). The average temperatures are also reported

cutoff for the wavefunction was set to 80 Ry, the time step was set to 4 a.u., and the fictitious mass for the orbital was chosen to be 400 a.m.u. In the present study we have used dispersion-corrected atom-centered pseudopotentials (DCACPs) [46] in the Troullier–Martins [47] format for oxygen and hydrogen. Norm-conserving Goedecker pseudopotentials [48–50] have been used for chloride. Production runs of 15 ps in the microcanonical ensemble followed an NVT equilibration run of 3 ps. The initial configuration was taken from classical molecular dynamics simulations. Ionic and molecular dipole moments were computed using the Wannier center [51, 52] analysis as explained in [23, 53].

2.4 Computed properties

The trajectories from both classical and Car–Parrinello MD have been post-processed in order to compute the following dynamical properties:

1. *ion diffusion*: chloride diffusion was studied computing the ion mean square displacement $\Delta_r(t)$ and velocity autocorrelation function $C_v(t)$ as

$$\Delta_r(t) = \langle [\mathbf{r}(t) - \mathbf{r}(0)]^2 \rangle, \tag{7}$$

$$C_v(t) = \frac{\langle \mathbf{v}(t) \cdot \mathbf{v}(0) \rangle}{\langle v^2(0) \rangle}. \tag{8}$$

the diffusion coefficient was obtained by calculating the slope of the $\Delta_r(t)$ and the integral of $C_v(t)$ as

$$D_{\mathrm{msd}} = \frac{1}{6} \lim_{t\to\infty} \frac{\mathrm{d}}{\mathrm{d}t} \Delta_r(t), \tag{9}$$

$$D_{\mathrm{vacf}} = \frac{k_{\mathrm{B}}T}{m} \int_0^\infty C_v(t)\mathrm{d}t. \tag{10}$$

2. *residence time of first shell molecules*: water molecules on the first shell could escape from there and then be substituted by outer molecules; this exchange process is quite fast for chloride, and the mean residence time of water molecules in the first shell could be evaluated from

$$n(t) = \left\langle \frac{1}{N_{1\mathrm{st}}} \sum_{i=1}^{N_{1\mathrm{st}}} \theta_i(t)\theta_i(0) \right\rangle, \tag{11}$$

where the sum runs over the $N_{1\mathrm{st}}$ hydration molecules present in the first shell at $t = 0$, θ_i is unity if the ith molecule is in the first shell, and it is zero otherwise. Given the high lability of the first hydration shell, $n(t)$ is evaluated by allowing first shell molecules to leave the first shell for a maximum period of time t^*. As in previous works [54], we used $t^* = \infty$. The resulting function could be fitted with a double exponential function $\tilde{n}(t) = A\exp(-k_1 t) + (1-A)\exp(-k_2 t)$. The integral of this function yields the characteristic residence time:

$$\tau_{1\mathrm{st}} = \int_0^\infty n(t)\mathrm{d}t, \tag{12}$$

where the integral was evaluated numerically up to $t = 5$ ps using $n(t)$ and analytically up to $t = \infty$ using $\tilde{n}(t)$.

3. *rotation of molecules in the first shell*: the study of reorientational motions has been carried out by means of the time correlation function $C_2^{\mathrm{OH}}(t)$ defined as follows:

$$C_2^{\mathrm{OH}}(t) = \langle P_2(\mathbf{u}_{\mathrm{OH}}(t) \cdot \mathbf{u}_{\mathrm{OH}}(0)) \rangle \tag{13}$$

where $\mathbf{u}_{\mathrm{OH}}$ is the unitary vector along the O–H bond of water molecules, and P_2 is the second Legendre polynomial, that is, $P_2(\cos\theta) = \frac{1}{2}(3\cos^2\theta - 1)$. This correlation function shows a "backscattering-like" minimum, known as the free rotor frequency, and then decays exponentially. The long-time decay can be fitted with a single exponential function $\tilde{C}_2^{\mathrm{OH}}(t) = A\exp(-kt)$. In order to interpret the $C_2^{\mathrm{OH}}(t)$ function, it is convenient to calculate its time integral, yielding the so-called reorientational correlation time

$$\tau_2^{\mathrm{OH}} = \int_0^\infty C_2^{\mathrm{OH}}(t)\mathrm{d}t, \tag{14}$$

which basically indicates the mean time employed by a water molecule to rotate around the O–H direction. The above integral was calculated numerically up to $t = 5$ ps using $C_2^{\mathrm{OH}}(t)$ and then analytically up to $t = \infty$ using $\tilde{C}_2^{\mathrm{OH}}(t)$.

4. *hydration shell rotation*: analogously to the previous one, the solvation shell rotation around the ion can be characterized by computing the time correlation function $C_2^{\mathrm{OCl}}(t)$ where in Eq. 13 the unitary vector along O–H bond is substituted by the unitary vector joining the chloride ion to oxygen atoms $\mathbf{u}_{\mathrm{OCl}}$. The rotational time of the solvation shell τ_2^{OCl} was evaluated as in Eq. 14.

Comparing the above dynamical properties with experimental data would require the description of zero point energy contributions with path integral techniques [55, 56]. Nevertheless, since the focus of the present contribution is on the capabilities of classical force field to reproduce dynamical properties of density functional based simulations, neither our classical nor Car–Parrinello MD simulations account for nuclear quantum effects.

3 Results and discussion

The diffusion of a solute is connected to its interaction with the solvent, particularly with the first-shell molecules. For ions in water, it has been shown that there exists a tight coupling between equilibrium and non-equilibrium effects of hydration shell exchange and ion diffusion [57]. Furthermore, in case of halide anions, a proper modeling of the interaction potential is of high importance for reproducing the hydrogen bonds, as the first hydration shell seems to be critically dependent on them. In Fig. 1 the mean square displacement (MSD) of the ion from CP and classical MD simulations are shown. For the sake of clarity, we show the results in three panels, each containing the MSD of potential models with a fixed value of anion polarizability (the same approach is used also for the following figures). It can be noticed that the MSD obtained in CPMD simulations is not as straight as the one computed in classical simulations. This is due to the shortness of CPMD trajectories which do not allow to gather enough statistics for the MSD. A similar effect was found for the velocity autocorrelation functions (not shown here). Nevertheless, a general trend could be appreciated in the graphs: For low values of the anion polarizability, the diffusion is slower than in the case of high polarizability. In Table 2 the values for the diffusion coefficients are shown. It can be noticed that the difference between exponential and gaussian damping functions correlates well with the difference in temperatures. Nonetheless, the potentials with exponential damping seem to perform slightly better than the ones with gaussian damping.

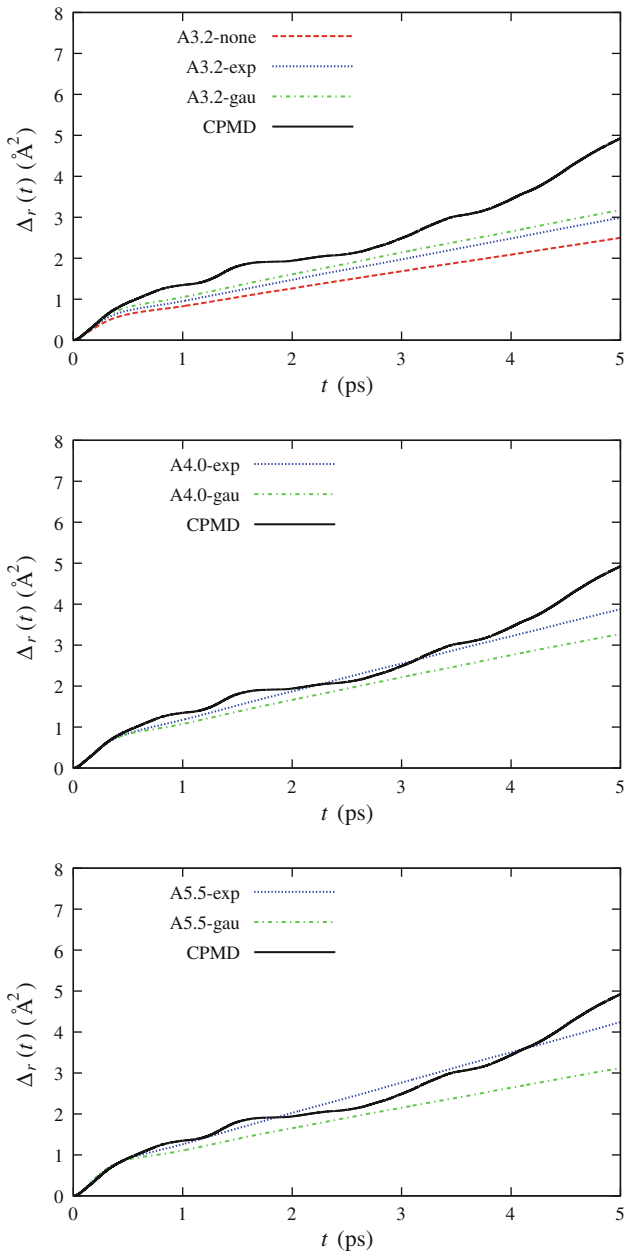

Fig. 1 Chloride mean square displacement of all models compared to Car–Parrinello results (key in the legend of each *panel*)

The lower ion mobility can be explained by considering that the interaction of ion with water dipole moments is badly described when a low polarizability value is taken as reference. In the case of undamped potentials, the induced dipole moment on the ion is much higher than in ab initio calculations. Therefore, high dipolar interactions render the system more viscous. In the case of damped potentials, the dipole moment is lower than the ab initio one at all distances. Hence the Coulomb interaction prevails upon the dipolar one, causing the hydrogen bond to be stronger and to slower the system dynamics. This is confirmed by the inspection of hydration shell exchange and rotational dynamics in Figs. 2, 3 and 4, and in Table 3. The residence time correlation function of first shell molecules decays much faster for high polarizability rather than for low polarizability. In the case of the exponential damping with high anion polarizability, the correlations function overlaps almost completely with CPMD results. A similar trend is observed in the rotational times of first shell molecules around the O–H bond. This measure is intimately connected to the hydrogen bond dynamics of first shell molecules with the anion. It can be seen that the correlation functions (Fig. 3) resemble the CPMD results better for high values of the polarizability.

As mentioned in the introduction, in a previous article, we showed that a higher polarization anisotropy of the first solvation shell is associated with a low anion polarizability. This has a direct consequence on the collective motion of first shell molecules. The rotational correlation function of the Cl–O bond (Fig. 4) conveys a picture of how fast the whole solvation shell rotates around the ion. Again, only at high values of the anion polarizability, we recover the dynamical behavior of ab initio simulations.

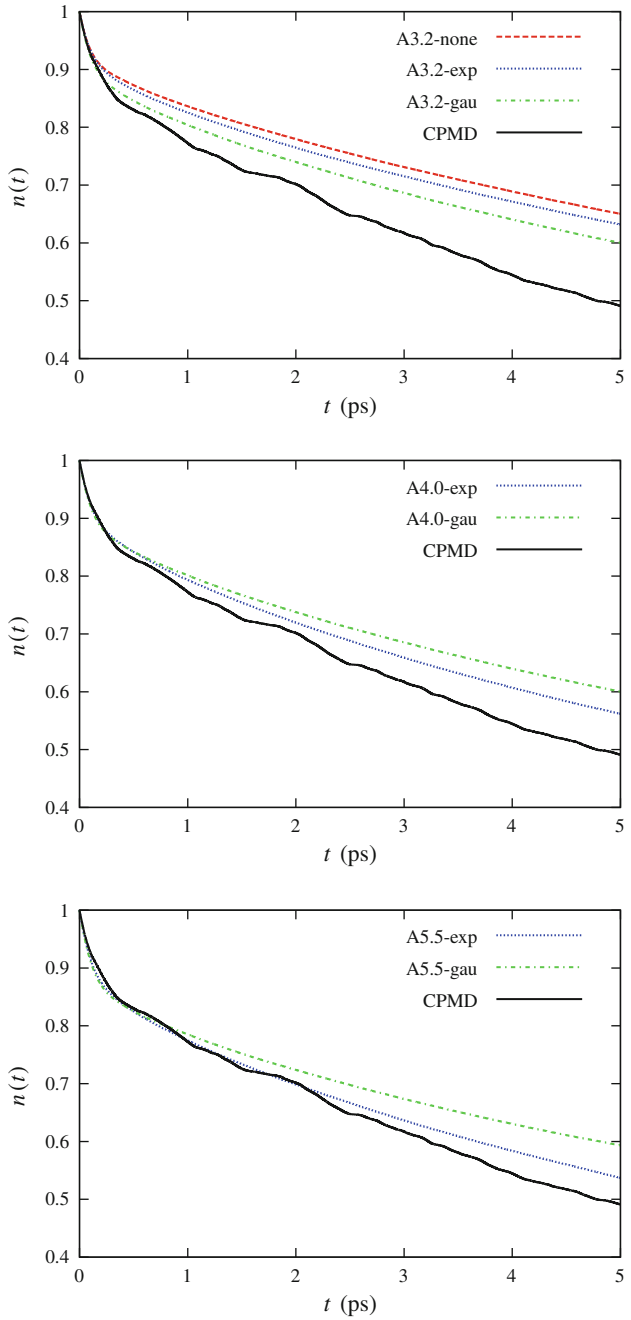

Fig. 2 First shell residence correlation function of all models compared to Car–Parrinello results (key in the legend of each *panel*)

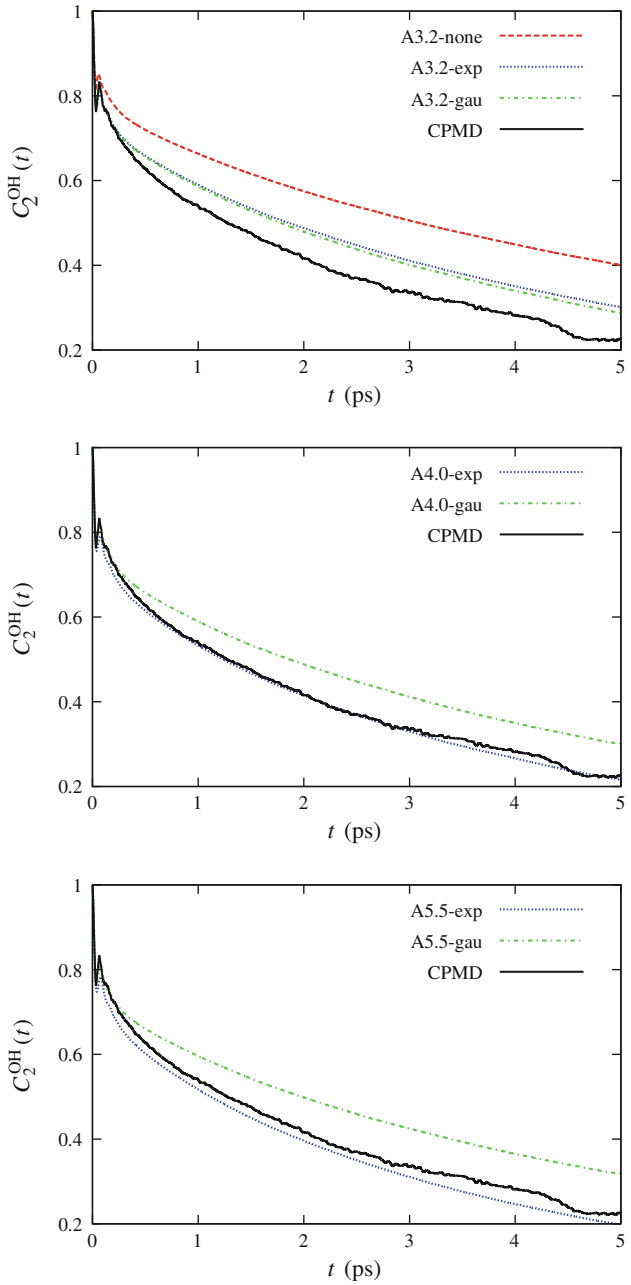

Fig. 3 O–H reorientational correlation functions for the first shell water molecules. Results for second Legendre polynomial are shown for all models, compared to Car–Parrinello results (key in the legend of each *panel*)

From the above results we learn that the ion solvation dynamics is well reproduced by a system with high anion polarizability. Using a low polarizability seems to dampen the dynamics and to render it slower, at least for the motions studied here. Moreover it seems that the exponential damping performs slightly better than the gaussian one. Nonetheless we would like to remark that the damping parameters were not optimized for condensed-phase simulations. Thus, it is not correct to conclude that, *always*, the exponential damping performs better than the gaussian one; in fact it is only in the case of our parameter set. Finally it can be seen that the results obtained for polarizability values equal to 4 and 5.48 $Å^3$ do not differ very much, the main difference lying in the decay of the exchange correlation function. From this result it would be tempting to use the anion polarizability equal to 4 $Å^3$; it must be highlighted, though, that statical properties are not as well reproduced for A4.0-gau and A4.0-exp model potentials (see [28]). Therefore, since it is highly important

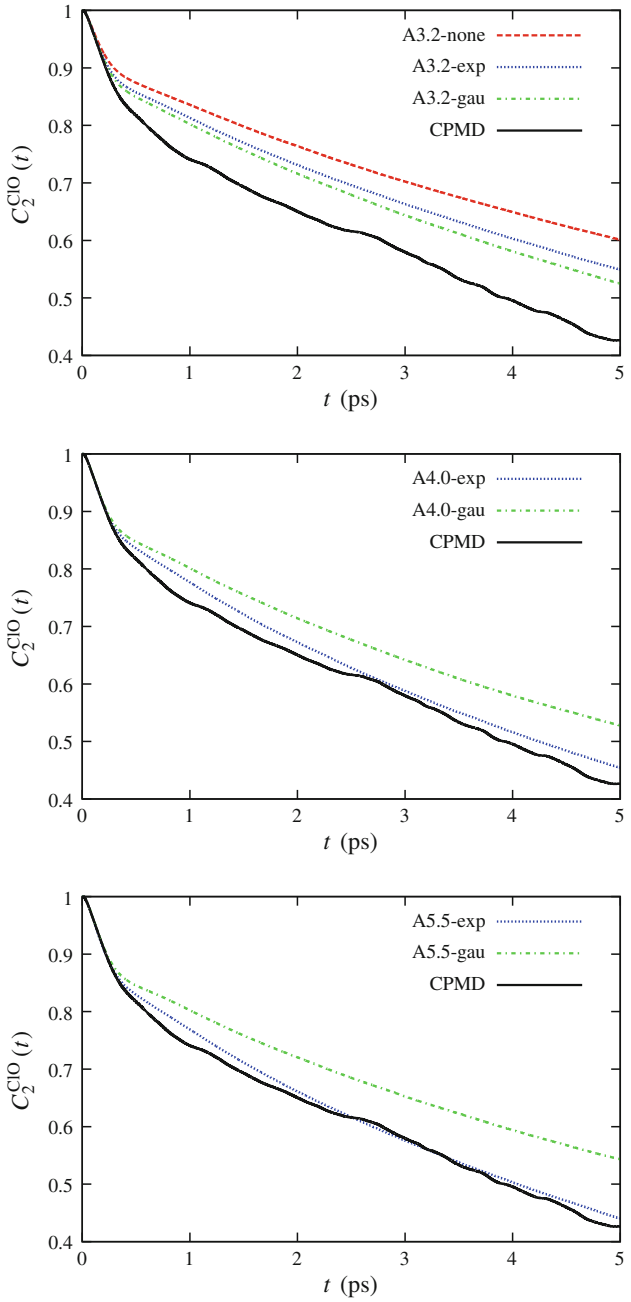

Fig. 4 O–Cl reorientational correlation functions for the first shell water molecules. Results for second Legendre polynomial are shown for all models, compared to Car–Parrinello results (key in the legend of each *panel*)

to reproduce faithfully both static and dynamical properties, we suggest the use of A5.5-gau and A5.5-exp force fields, or similar (optimized) ones with the value of the anion polarizability equal to 5.48 $\mathring{A}^3$.

In the above discussion we have never mentioned the role played by water polarizability. The water model is certainly important when considering the solvation shell dynamics; nevertheless it should be observed that the anion shows higher fluctuations in the dipole moment (from almost 0 to 2 Debye), which are relevant in driving the system dynamics. We acknowledge, though, that a better force field for water is needed; we are currently working on this topic.

4 Conclusions and perspectives

The use of damping functions for the simulation of polarizable systems has been introduced since 1981 [26]. The main reason to include *intra-molecular* damping has been the need to hinder the polarization catastrophe for simulations with the polarizable point dipoles method. Though, until few years ago, electrostatic damping was not used to treat also *inter-molecular* interactions; probably this delay was due to the fact that the electric fields in most of the studied systems were not high enough to cause any appreciable divergence of the dipoles. In 2005, by studying a simple ion–water dimer, it was found that the damping of inter-molecular electrostatic interactions was needed to reproduce short-range effects of interacting electron densities [21]. In the case of highly polarizable ions, such as halides, it was remarked that, to reproduce both long- and short-range polarization, the damping functions should be used on top of force field where the halide had its gas-phase polarizability [22].

Recently we showed that the latter conclusion holds also for the case of chloride in bulk water; ab initio results on the static properties of this system were nicely reproduced using the same polarizability and damping functions optimized for gas-phase calculations [28].

In this contribution we showed that the same force field allows to reproduce better also dynamical properties of the ion and of its solvation shell. It seems that, in the absence of damping functions, the dynamics of chloride and of first shell molecules is slower. Therefore, the introduction of damping functions is highly important when studying dynamical properties. Both exponential and gaussian charge distributions yield good results, the former performing slightly better than the latter. It must be stressed that the force field was not parameterized using the above properties as target in any optimization procedure. Thus, it seems that the results have a broad range of validity and that the force field parameters used are portable from gas to condensed phase.

The calculation of damping functions implies a negligible computational overhead, and it can be easily ported also to other methods to include polarizability. In fact, it suffices to use the appropriate screening functions in the electrostatic interaction tensors (Eq. 1). The application to shell models at gas and condensed phase could be found in [21, 38, 39].

Table 3 Residence time, and O–H and O–Cl reorientational correlation times of the first shell molecules

Model	τ_{1st} (ps)	τ_2^{OH} (ps)	τ_2^{ClO} (ps)
A3.2-none	14.0 (1.3)	6.2 (0.5)	11.3 (0.9)
A3.2-exp	13.2 (2.0)	4.4 (0.9)	9.5 (1.7)
A3.2-gau	11.6 (0.7)	4.1 (0.5)	8.6 (0.9)
A4.0-exp	9.9 (1.3)	3.0 (0.3)	6.8 (0.9)
A4.0-gau	11.8 (1.4)	4.3 (0.5)	8.8 (1.2)
A5.5-exp	9.1 (0.5)	2.8 (0.2)	6.4 (0.4)
A5.5-gau	11.9 (1.8)	4.6 (0.7)	9.4 (1.5)
CPMD	7.5	3.0	6.0

Values for classical MD are averaged over six NVE simulations (mean standard deviations in parenthesis)

Finally we would like to address a subtle issue arising from the above conclusions. On the one hand, we showed that, using gas-phase polarizability with the appropriate damping functions allows to reproduce many static and dynamical properties compared to ab initio results. On the other hand, the use of gas-phase polarizability at condensed phase could seem nonsense; in fact, it is usually assumed that, in the bulk, the polarizability is lower than at gas phase. Whether the polarizability is an intrinsic property has still to be answered. What we have shown here is that, merely from the operative point of view, considering it an intrinsic property allows for a better description of structural and dynamical properties.

Acknowledgments The authors thankfully acknowledge the computer resources, technical expertise and assistance provided by the Barcelona Supercomputing Center - Centro Nacional de Supercomputación for the projects QCM-2009-1-0014, QCM-2008-3-0012 and QCM-2008-2-0010. The research institution INSTM is also acknowledged by M.M., who is also thankful for the resources given by the *Cybersar Project* managed by the "Consorzio COSMOLAB". E.G. acknowledges financial support from the Direcció General de Recerca de la Generalitat de Catalunya (Grant 2009SGR-1003) and from the Ministerio de Ciencia e Innovación (MICINN) of Spain (Grant FIS2009-13641-C02-01).

References

1. Jorgensen WL (2007) J Chem Theory Comput 3:1877
2. Iuchi S, Izvekov S, Voth GA (2007) J Chem Phys 126:124505
3. Piquemal JP, Perera L, Cisneros GA, Ren P, Pedersen LG, Darden TA (2006) J Chem Phys 125:054511
4. Jiao D, King C, Grossfield A, Darden TA, Ren P (2006) J Phys Chem B 110:18553
5. Rick SW, Stuart SJ (2002) Rev Comp Chem 18:89
6. Burnham CJ, Li J, Xantheas SS, Leslie M (1999) J Chem Phys 110:4566
7. Stone AJ (2008) Science 321:787
8. Jungwirth P, Tobias DJ (2006) Chem Rev 106:1259
9. Kuo IFW, Mundy CJ (2004) Science 303:658
10. Wick CD, Xantheas SS (2009) J Phys Chem B 113:4141
11. Wick CD (2009) J Chem Phys 131:084715
12. Duvail M, Vitorge P, Spezia R (2009) J Chem Phys 130:104501
13. Hull S, Keen DA, Madden PA, Wilson M (2007) J Phys Cond Matter 19:406214
14. Bitrian V, Trullas J (2008) J Phys Chem B 112:1718
15. Krekeler C, Dommert F, Schmidt J, Zhao YY, Holm C, Berger R, Delle Site L (2010) Phys Chem Chem Phys 12:1817
16. Harder E, Mackerell AD, Roux B (2009) J Am Chem Soc 131:2760
17. Masia M, Probst M, Rey R (2004) J Chem Phys 121:7362
18. Lopes PEM, Roux B, MacKerell AD (2009) Theor Chem Acc 124:11
19. Kaminski GA, Stern HA, Berne BJ, Friesner RA (2004) J Phys Chem A 108:621
20. Giese TJ, York DM (2005) J Chem Phys 123:164108
21. Masia M, Probst M, Rey R (2005) J Chem Phys 123:164505
22. Masia M, Probst M, Rey R (2006) Chem Phys Lett 420:267
23. Masia M (2008) J Chem Phys 128:184107
24. Piquemal JP, Chelli R, Procacci P, Gresh N (2007) J Phys Chem A 111:8170
25. Söderhjelm P, Öhrn A, Ryde U, Karlström G (2008) J Chem Phys 128:014102
26. Thole BT (1981) Chem Phys 59:341
27. Souaille M, Loirat H, Borgis D, Gaigeot MP (2009) Comp Phys Commun 180:276
28. Sala J, Guàrdia E, Masia M (2010) J Chem Phys 133:234101
29. Smith JD, Saykally RJ, Geissler PL (2007) J Am Chem Soc 129:13847
30. Bakker HJ (2008) Chem Rev 108:1456
31. Mallik BS, Semparithi A, Chandra A (2008) J Chem Phys 129:194512
32. Omta AW, Kropman MF, Woutersen S, Bakker HJ (2003) Science 301:347
33. Laage D, Hynes JT (2007) Proc Natl Acad Sci USA 104:11167
34. Masia M, Rey R (2005) J Chem Phys 122:094502
35. Kropman MF, Nyenhuys HK, Bakker HJ (2002) Phys Rev Lett 88:77601
36. Kropman MF, Bakker HJ (2001) Science 291:2118
37. Stone AJ (1996) The theory if intermolecular forces. Clarendon Press, Oxford
38. Lamoureux G, Roux B (2006) J Phys Chem B 110:3308
39. Harder E, Anisimov VM, Whiteld T, MacKerrell AD, Roux B (2008) J Phys Chem B 112:3509
40. Dang LX (1992) J Chem Phys 97:2659
41. Kolafa J (2004) J Comp Chem 25:335
42. Car R, Parrinello M (1985) Phys Rev Lett 55:2471
43. Copyright IBM Corp. 1990–2006, computer code CPMD version 3.11, (MPI für Festköorperforschung Stuttgart 1997–2001)
44. Becke AD (1988) Phys Rev A 38:3098
45. Lee C, Yang W, Parr RG (1988) Phys Rev B 37:785
46. Lin IC, Seitsonen AP, Coutinho-Neto MD, Tavernelli I, Rothlisberger U (2009) J Phys Chem B 13:1127
47. Troullier N, Martins JL (1991) Phys Rev B 43:1993
48. Goedecker S, Teter M, Hutter J (1996) Phys Rev B 54:1703
49. Hartwigsen C, Goedecker S, Hutter J (1998) Phys Rev B 58:3641
50. Krack M (2005) Theor Chem Acc 114:145
51. Marzari N, Vanderbilt D (1997) Phys Rev B 56:12847
52. Silvestrelli PL, Parrinello M (1999) Phys Rev Lett 82:3308; erratum: (1999) Phys Rev Lett 82:5415
53. Guàrdia E, Skarmoutsos I, Masia M (2009) J Chem Theory Comput 5:1449
54. Guàrdia E, Laria D, Martí J (2006) J Phys Chem B 110:6332
55. Paesani F, Iuchi S, Voth GA (2007) J Chem Phys 127:074506
56. Paesani F, Yoo S, Bakker HJ, Xantheas SS (2010) J Phys Chem Lett 1:2316
57. Møller KB, Rey R, Masia M, Hynes JT (2005) J Chem Phys 122:114508